NeuroImage **16,** 115–129 (2002)
doi:10.1006/nimg.2002.1065, available online at http://www.idealibrary.com on IDEAL®

Brain Activation Sequences Following Electrical Limb Stimulation of Normal and Paraplegic Subjects

Andreas A. Ioannides,* Lichan Liu,* Ara Khurshudyan,* Roger Bodley,† Vahe Poghosyan,* Tadahiko Shibata,* Jürgen Dammers,‡ and Ali Jamous†

**Laboratory for Human Brain Dynamics, Brain Science Institute (BSI), RIKEN, 2-1 Hirosawa, Wako-shi, Saitama, 351-0198, Japan; †Stoke Mandeville Hospital, Aylesbury, Buckinghamshire, HP21 8AL, United Kingdom; and ‡Institute of Medicine, Research Center Jülich, D-52425 Jülich, Germany*

Received April 2, 2001

In current clinical practice the degree of paraplegia or quadriplegia is objectively determined with transcranial magnetic stimulation (TMS) and somatosensory-evoked potentials (SSEP). We measured the MEG signal following electrical stimulation of upper and lower limbs in two normal and three clinically complete paraplegic subjects. From the MEG signal we computed distributed estimates of brain activity and identified foci just behind the central sulcus consistent in location with primary somatosensory (SI) for arm and foot and secondary somatosensory (SII) areas. Activation curves were computed from regions of interest defined around these areas. Activation of the SI foot area was observed in normal and paraplegic subjects when the upper limb was stimulated. Surprisingly, for each paraplegic subject, stimulation below the lesion was followed by cortical activations. These activations were weak, only loosely time-locked to the stimulus and were seen intermittently behind the central sulcus and nearby cortical areas. Statistical analysis of tomographic solutions and activation curves showed consistent responses following foot stimulation in one paraplegic (PS1) and intermittently in another paraplegic subject. We repeated the same experiment for PS1 in a different laboratory and the results from the analysis of foot stimulation from both laboratories revealed statistically significant focal cortical response only in the contralateral SI foot area. © 2002 Elsevier Science (USA)

Key Words: **spinal cord injury (SCI); magnetoencephalography (MEG); cortical plasticity; somatosensory cortex; electrical stimulation.**

INTRODUCTION

Spinal cord injury (SCI) following trauma leading to residual neurological disability affects millions of people worldwide, e.g., there are an estimated 250,000 SCI individuals living in the U.S. Patients with clinically complete paraplegia are unable to perceive any sensation or to effect any motor control or movement in that part of the body innervated below the lesion, although the brain areas that used to be closely associated with sensation and movement of the body below the lesion are still intact. There is still controversy surrounding treatment in the acute stage (e.g., the role of surgical stabilization and high dose intravenous steroids) and currently there is no accepted treatment in the chronic stage apart from the treatment of complications such as spasticity, pain, and syringomyelia. In contrast to the situation in peripheral nerves, lesions in the mammalian central nervous system (i.e., brain and spinal cord) cannot be repaired (Nicholls *et al.,* 1999). However, there is increasing understanding of the mechanical and neurohumoral factors that inhibit or prevent spinal cord axonal regeneration and therapeutic repair or grafting appears increasingly possible (McDonald, 1999; Whittemore, 1999; Keirstead and Blakemore, 1999). Therefore it is considerably important in ascertaining if activity associated with the unaffected parts of the body invades these areas and in being able to monitor any new activity that might follow such regeneration process.

Advances in neuroimaging techniques in recent years made it possible to study the changes in brain activity in SCI patients. Using positron emission tomography (PET), SCI patients at rest showed lower global absolute glucose metabolism than normal controls but relatively increased glucose metabolism in areas involved in movement initiation and attention (Roelcke *et al.,* 1997). Further, a recent PET study (Bruehlmeier *et al.,* 1998) showed that during hand movement SCI patients exhibited an expansion of the cortical hand area towards the leg area, with an enhanced bilateral activation of the thalamus and cerebellum. Magnetic resonance imaging (MRI) is now well established for assessing spinal-cord damage in both acute and chronic situations, while functional MRI (fMRI) has also been used to investigate reorganization in primary motor cortex in SCI patients (Lotze *et al.,*

1053-8119/02 $35.00

TABLE 1A

Paraplegic Subjects' Details

Subject	Age (years)	Level	ASIA	Duration (years)	Cause	Medication
PS1 (J&R)	46	T6	A	29	MVA	Diazepam 5 mg daily; Baclofen 10 mg twice daily
PS2 (J)	43	T10	A	3	MVA	Oxybutenene 25 mg daily
PS3 (J)	36	T11	A	14	Fall	None

Note. Subject, Subject index and recording sites (J, Jülich; R, RIKEN). Age, age at the time of MEG recording in Jülich. ASIA, American Spinal Injury Association Impairment scale. Duration, years of SCI at the time of MEG recording in Jülich. MVA, motor vehicle accident.

1999). Lotze *et al.* reported that patients with complete paraplegia showed a cranial displacement of activation in the contralateral primary motor cortex during elbow but not thumb and lip movement. Transcranial magnetic stimulation (TMS) has also revealed changes in the brain activity in SCI patients (Levy *et al.*, 1990; Topka *et al.*, 1991; Streletz *et al.*, 1995; Alexeeva *et al.*, 1997, 1998; Calancie *et al.*, 1999; Smith *et al.*, 2000). A reorganization of the motor cortex of a patient with complete loss of right hand function following traumatic avulsion of the cervical roots C7 and C8 was demonstrated by a combined fMRI and TMS study (Foltys *et al.*, 2000). Both fMRI and TMS showed an expansion of the motor representation of the forearm into the hand area of the contralateral to the injured side. Activation of the hand area was nevertheless observed with fMRI when the patient was instructed to imagine finger tapping with his plegic hand.

Both the PET and fMRI techniques use indirect markers, i.e., glucose metabolism in PET and regional blood flow and/or deoxygenation in fMRI, to provide heamodynamic measure of the changes in brain activity in a time scale ranging from a few seconds to minutes. Electroencephalography (EEG) is another possible technique for detecting changes in the brain. A recent EEG study showed cortical sensorimotor and motor reorganization after SCI (Green *et al.*, 1998, 1999). EEG has good temporal but poor spatial resolution due to the its sensitivity to the conductivity profile of the human head (scalp, skull, and brain). Magnetoencephalography (MEG) has as good temporal resolution as EEG and is almost unaffected by the conductivity of the head. However, both EEG and MEG are governed by an ill-posed mathematical inverse problem, which poses a formidable theoretical problem but a less severe one in practice. For focal superficial generators, like SI and SII areas, changes in location of a few mm can be reliably identified.

The aim of our study was to evaluate both quantitatively and qualitatively the changes in brain activity in SCI patients by comparing with matched normal subjects. A subset of the subjects was studied with two different MEG systems as part of a replication test. Electrical stimulation was applied to the wrists (innervated above the lesion) and ankles (innervated below the lesion) of both subject groups. Magnetic field tomography (MFT) was used to extract the evoked brain response millisecond by millisecond and to address two critical aspects of the quality of estimates of brain activity: localization accuracy and statistical significance.

MATERIALS AND METHODS

Subjects

One left-handed and four right-handed males were selected from a large pool of paraplegics attending the National Spinal Injuries Center, Stoke Mandeville Hospital, UK. The criteria for the selection included a stable, clinically complete paraplegia due to a posttraumatic spinal cord lesion, no metal implant or fixation surgery and a full agreement to undergo the rigors of a journey to Germany and the 2-day MEG and MRI recordings. The paraplegic subjects selected for the study underwent further clinical and neurophysiological examination for research purposes prior their travel for the experiment. The lesions were confirmed as complete by standard electrophysiological techniques as described in Appendix A.

The original protocol and the wider schedule for handling the transport of the patients by car or plane from their home in the UK to Jülich and back and the comfortable and convenient stay while in Jülich was considerably changed after the first paraplegic subject (left-handed) was examined. The modified protocol worked well for the remaining four paraplegic and three matched normal subjects. However, because of strong and persistent artifacts, we excluded one normal and one paraplegic subject for further analysis. The remaining five subjects were all right-handed. Average age was 41.7 $\pm$ 5.1 years (mean $\pm$ SD) for the three paraplegic subjects (PS1-3) and 48.5 $\pm$ 3.5 years for the two normal subjects (NS1-2). More details for the three paraplegic subjects are given in Table 1a. One of the three paraplegic subjects (PS1) and the two normal subjects (NS1-2) repeated the experiment using a different whole-head MEG system at RIKEN (Japan).

TABLE 1B

Applied Intensity Values (in mA) for Paraplegic Subjects

Stimulus / Subject	Right arm weak	Right arm strong	Left arm weak	Left arm strong	Right foot weak	Right foot strong	Left foot weak	Left foot strong
PS1	6 (4.9)	15 (9.8)	7 (5)	20 (10.3)	14 (4)	40 (14)	14 (4)	40 (14)
PS2	5.4	16.3	3.6	17	10	22	10	22
PS3	6	19.5	4.8	18.8	10	25	10	25

Note. For PS1 the numbers in brackets show the intensity values used in the Riken experiment. All other numbers correspond to the Jülich experiment.

Before each experiment all details of the experiment were explained and the subjects read a written description before signing the informed consent form in accordance with the Declaration of Helsinki.

MEG Signal Recording and Processing

Experiment 1 (Jülich). The BTi whole head system (148 channels) was used to record MEG signals from the five subjects during electrical limb stimulation. Electrical pulses at two different stimulation levels (duration 0.2 ms, interstimulus interval (ISI) 1.0 $\pm$ 0.1 s) were applied in turn to the left and right median nerves at the wrist and the tibial nerves at the ankle (Table 1b). One hundred and three hundred trials were delivered at the strong and weak levels, respectively. The intensity levels were adjusted to different values based on the subject feedback before and fixed throughout the experiment. During the recording, the subjects were instructed to relax and keep their eyes open fixating on a small green circular mark ahead. The electrical pulses were generated using a DIGITIMER constant current high voltage stimulator (model DS7A).

The MEG signal was recorded in epoch mode, 300 ms before the onset of the stimuli for 800 ms, sampled at 1017.25 Hz, with an online filter of 0 to 400 Hz. For each limb and stimulation level, the MEG signal was recorded in a separate run (8 runs in total). We also recorded the background MEG signals when the subject was in place but no stimulation was applied in a continuous mode for 5 min. Two such subject baseline measurements were taken before and after the main experiment, with the data sampled around a trigger event generated internally by the BTi hardware.

For each run, the standard BTi noise reduction was first used to reduce environmental noise. The procedure relied on coefficients with fixed weights to compute external noise still penetrating the shielded room from measurements recorded from reference channels in the dewar. The "noise-free" signal was further digitally band-pass filtered in the 1–200 Hz range with notch filters at 50, 100, and 150 Hz, using the standard BTi software (Infinite Impulse Response Butterworth filters, filter order 2). Finally the average signal was constructed based on the onset of the stimulation.

Experiment 2 (Riken). The experiment protocol was made as similar as possible to that used in Jülich. The stimulus lasted for 0.2 ms with ISI of 1.0 s (Grass stimulator model S8800). The stimulation levels were determined by the subject's sensation (just felt; S) and movement (clear twitches observed; M) levels. The weak level was defined as $S + 0.25 \times (M - S)$, while the strong level was $M + 0.25 \times (M - S)$. Two runs were recorded for each limb at either stimulation level (Table 1b). One hundred and 300 trials were delivered at the strong and weak levels, respectively.

The MEG signal was recorded using the whole-head CTF system (151 channels) at a sample rate of 1250 Hz with an online filter of 0–200 Hz. The signal was then filtered offline at 1.25–200 Hz and averaged on the onset of stimulation separately for each run.

MEG Signal Analysis

We used magnetic field tomography (MFT) to compute the 3-D distribution of activity throughout the brain. MFT produces probabilistic estimates for the (nonsilent) primary current density vector $\vec{J}^p(r, t)$ from a given distribution of MEG data (Ioannides *et al.*, 1990; Ioannides, 1995a). The MFT algorithm relies on a nonlinear solution to the inverse problem, where the sensitivity profile of the sensors is used as an expansion basis for the direction of the primary current density. A weighted expansion is used, with the *a priori* probability weight determined through a training session from computer generated data. For each experimental arrangement (i.e., for each run and subject) a different *a priori* probability weight is used, determined by a separate training session. The *a priori* probability weight is then fixed for the analysis of the real data. The MFT algorithm was developed through simulations where a family of algorithms were tested and arranged according to the power law dependence of the *a priori* probability weight on the modulus of the unknown current density. Empirical support for MFT has been provided in numerous applications (Ioannides, 1995a; Ioannides *et al.*, 1995b). The closest to a "gold standard" was an *in vivo* study (Ioannides *et al.*, 1993a), where the position and direction for a single implanted dipole and a pair of fairly deep implanted

dipoles were successfully extracted from the data. The MFT analysis of average signals was also in agreement with earlier studies using the equivalent current dipole model (Ioannides *et al.*, 1993b). A recent study of lead field expansions (Taylor *et al.*, 1999) has added strong mathematical justification, showing that MFT possesses the expected properties for localized distributed sources.

The average signal for the five subjects was analyzed from 200 before to 400 ms after the stimulation onset with the sample rate of 1.97 and 0.8 ms, respectively, for the Jülich and RIKEN data. For each subject, four hemispherical source spaces were defined, each covering the left, right, top and back part of the brain well. MFT was then used separately to extract brain activity from the MEG signal corresponding to the 90 channels closest to each of the four source spaces. The spatially overlapping estimates from the four source spaces were combined into one covering the entire brain. For display reasons, the reconstruction was displayed in 4913 ($17 \times 17 \times 17$) voxels, evenly distributed within the combined source space.

Post-MFT Analysis and ROI Definition

Since the MFT reconstruction was made completely independently for each timeslice and source space in each run, the pixel-by-pixel comparison was possible across different runs between post- and prestimulus periods for each subject. We performed the pixel-by-pixel comparison using the software STIMULATE (Strupp, 1996) in two stages. First, we identified statistically significant changes between pre and poststimulus period for each run. The modulus of the current density from the MFT solution was integrated over three timeslices (5.9 ms for Jülich and 2.4 ms for Riken data) from -150 to 150 ms. A separate statistical t-test map was then constructed for each run comparing the pre-stimulus (-150 to -50 ms) with poststimulus (20 to 150 ms) period. The poststimulus period was different for SI and SII areas reflecting their different onsets and waveforms. For paraplegic subjects the poststimulus window was further adjusted to allow for less precisely time-locked responses. Second, we identified the areas showing significant changes for each limb stimulation run by combining all the maps from the first stage across the same limb regardless of stimulation levels (weak and strong). For the subjects that participated in both sets of experiments the Jülich and Riken runs were also combined. We used the STIMULATE's threshold and logical functions in its Mask Generation procedure to combine maps from the same limb. All pixel values in each resulting map were set to zero except the ones with $P <$ 0.02 being set to one. The final statistical maps provided a much more robust and sensitive test than what was available in each individual map and produced only a few focal areas showing significant changes across the same limb stimulations. For instance, contralateral SI areas from the arm stimulation were identified for all five subjects and from the foot stimulation for the two normal and for the two of three paraplegic subjects (PS1 and PS2).

From the focal areas showing significant changes we defined regions of interest (ROI) as spherical regions with a radius of 1 cm for each subject. The ROIs were then displayed on the appropriate MRI brain slice of the subject and labeled accordingly. In order to compare results across subjects, the functionally defined ROIs for each subject were transformed into the Talairach coordinate (TC) system, and then back-transformed into the MRI coordinates of one normal subject (NS2) so that ROIs defined individually could be displayed on one common MRI background. The SI arm area was defined from the contralateral strong stimulation in each subject. In some subjects either left/right or both SII ROIs could not be defined functionally. The SII ROI was then defined by mirroring from the SII ROI of the other hemisphere if available. If no SII ROI could be defined by functional criteria the TC of the SII ROIs of the other subjects were averaged and then being back-transformed to the MRI coordinates of the subject. For instance, for PS3 no significant focal activations were identified by the analysis of the tibial nerve stimulation data. The foot ROI on the left hemisphere of PS3 was taken as the transformed (via TC) of the average of the other four subjects and this area was then mirrored to obtain the right SI foot area. In this paper, we shall limit our discussions to six ROIs, which were labeled based on anatomical structures, timing of prominent activations and the stimulated limb. The ROIs are left/right SI arm area during the median nerve stimulation and left/right SI foot area during the tibial nerve stimulation, and left/right SII area during both median and tibial nerve stimulation. The TCs of these 6 ROIs and the method used to define each are listed in Table 2. Figure 1 shows the six ROIs defined for normal subject NS2 in both sagittal and axial views, together with the top hemispherical source space and the corresponding selected 90 channels for the MFT reconstruction. For comparison, the six ROIs defined for the three paraplegic subjects are also projected and displayed on NS2's sagittal MRI slices by first transformation to the TC system and then back-transformation to the MRI coordinates of NS2. The figure shows the centers of the ROIs for the three paraplegic subjects are within or at the border of the 1-cm radius ROI for NS2.

Activation Curves and KS-Test

Once the ROI was defined the activation curve for each ROI could then be computed. Directional activation curves $\vec{J}_1(t)$, describing how the ROI activity

TABLE 2

The Talairach Coordinates (x, y, z, in mm) for the Six ROIs Defined in the Somotosensory SI and SII Areas, from the MFT Analysis of the Jülich Data

Subject	NS1			NS2			PS1			PS2			PS3		
ROI															
Left SI arm	−40	−32	56	−45	−20	57	−34	−32	56	−43	−21	58	−43	−24	58
Right SI arm	38	−30	55	47	−13	53	47	−11	44	37	−31	55	40	−23	51
Left SI foot	−3	−51	60	−12	−34	70	−2	−38	66	−11	−31	73	−6	−38	70^{O}
Right SI foot	8	−46	58	3	−35	70	14	−36	67	7	−37	70	6	−38	70^{M}
Left SII	−59	−21	24^{O}	−55	−14	18	−55	−10	18	−56	−10	16	−59	−18	23
Right SII	58	−13	28^{O}	54	−14	22	60	−6	17	56	−10	16^{M}	59	−18	23^{M}

Note. ^{M} Denotes the ROI defined by mirroring the ROI from the homologous hemisphere, while ^{O} represents the ROI obtained by averaging from other subjects.

changes along the main direction $\hat{e}_1$, was identified by a program for automatic scanning (Ioannides *et al.*, 1995b):

$$\vec{J}_1(t) = \iiint_{ROI} \vec{J}^{\,p}(\vec{r},\, t) \cdot \hat{e}_1 d^3r$$

Activation curves were also constructed for the modulus of the current density:

$$M(t) = \iiint_{ROI} \sqrt{\vec{J}^{\,p}(\vec{r},\, t) \cdot \vec{J}^{\,p}(\vec{r},\, t)}\, d^3r$$

Furthermore, we used the Kolmogorov–Smirnov (KS) test to identify time segments with statistically significant activations. The KS test uses the maximum difference between the target and baseline cumulative distributions to define the significance level, i.e., what is the probability that the target and baseline distributions are the same? We used the same variant of the test, which we called composite KS test that was previously employed with MFT solutions in a simple auditory task (Liu *et al.*, 1998) and in an object and emotion recognition task (Liu *et al.*, 1999). Multiple KS tests were applied for a given target distribution using a set of baseline distributions to allow for the rather variable nature of the electrophysiological activity. The highest *P* value was chosen as a conservative measure of significance. We used a window size of 21.6 ms and slided this window along the latency axis with a step of 1.97 ms. Each such window for each stimulation run defined a target distribution. The composite KS test was then used to compare each target distribution with each one of 15 baseline distributions (size 39.3 ms, step 39.3 ms) formed from the subject baseline run (no stimulation with the subject in place). In this way statistical significance could be assigned preserving both regional and dynamic richness of the MFT solutions.

RESULTS

Verbal Feedback

For median nerve stimulations, at the weak level both paraplegic and normal subjects could just feel the stimuli. The sensation was always felt and could be ignored easily (it had no annoyance value). At the strong level the stimulus induced involuntary twitches of the thumb and index finger, it was not painful but could not be ignored. For the tibial nerve stimulations, the normal subjects experienced twitches at the big toe (NS1) or small toe (NS2). For NS1 and NS2 weak and strong stimuli produced similar sensations in the lower limbs as the corresponding median nerve stimulations in the upper limbs. The paraplegic subjects felt nothing and no toe movement was observed, except for PS3, who reported vague sensation occasionally in his face or neck during stimulation. This sensation was intermittent and did not match the rate of the actual stimulation.

Jülich MEG Signals

Figure 2 compares the average MEG signal from NS2 and PS1 in the Jülich experiment. The figure shows that (1) The subject baseline signal was much weaker compared with the stimulation runs, except during the foot stimulation of PS1 when the signal strength of the baseline and stimulation runs was comparable. (2) For the strong arm stimulation in both subjects, the first peak was observed around 20–30 ms, followed by a prominent peak at around 80–90 ms. (3) For the strong foot stimulation of NS2, the first strong peak was around 40–50 ms and was followed by another dominant and stronger peak around 90–100 ms. In general, for all the five subjects, strong arm stimulation produced the strongest and sharpest MEG sig-

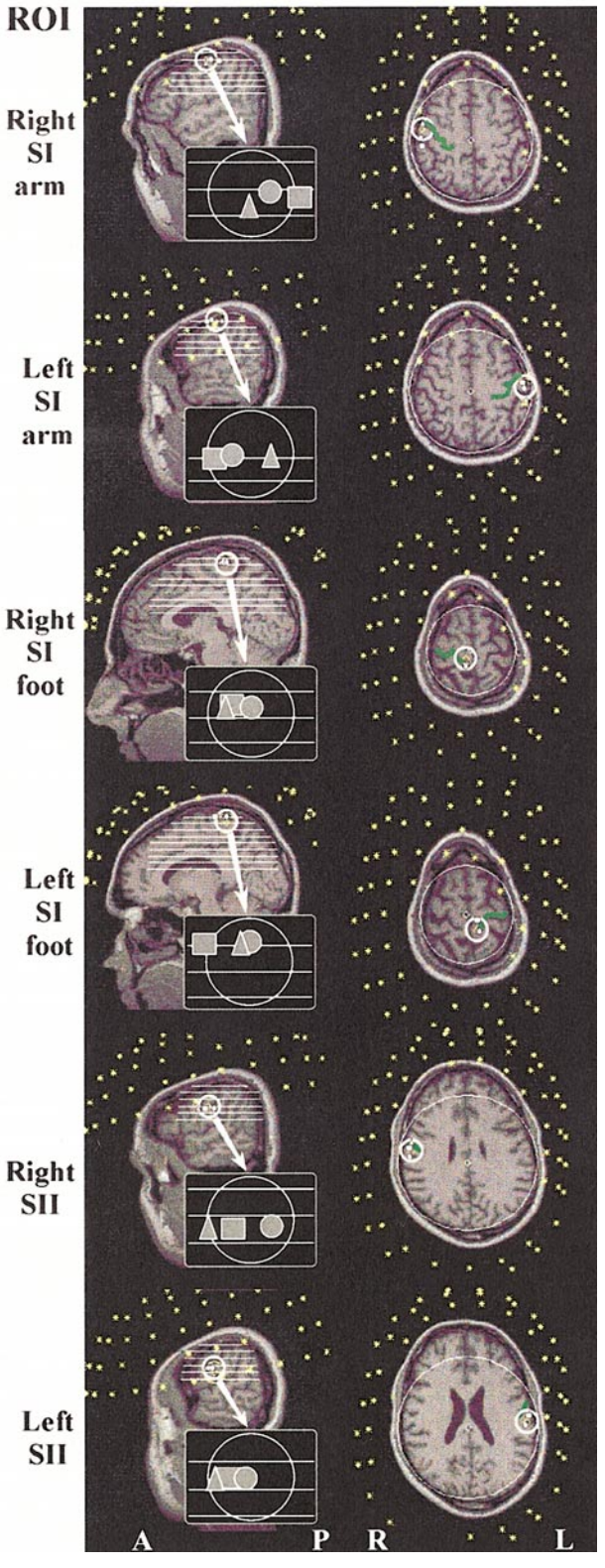

FIG. 1. The sensor locations and source space definition used for one of the MFT estimates (top hemispherical source space) for NS2: * denotes the 90 selected sensors, white lines in sagittal view and big circles in axial view show display cuts for the top source space. Small circles represent the ROI definitions and short green curves (in axial view) highlight the central sulcus. For comparison, the TC of the corresponding ROIs of the three paraplegic subjects are back-transformed into the MRI coordinates of NS2 and projected onto the displayed MRI slice. An insert shows the enlargement of the displayed ROIs, with ▲ for PS1, ■ for PS2, and ● for PS3.

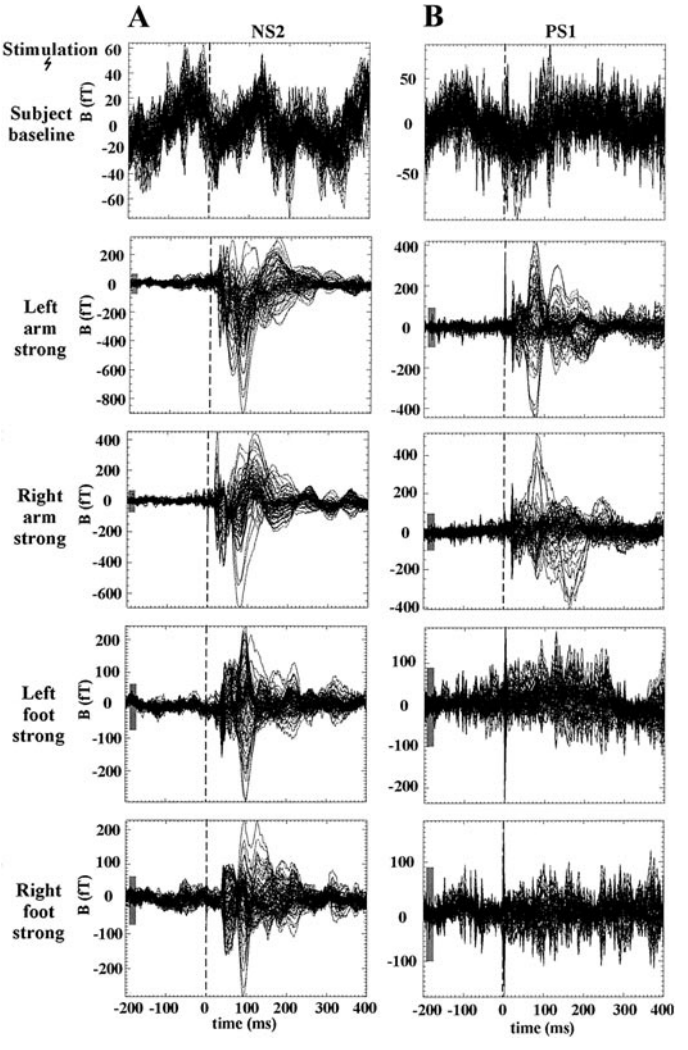

FIG. 2. Comparison of average MEG signals (Jülich) from the 90 sensors used for the top MFT computations from one normal (A) NS2 and one paraplegic subject (B) PS1, 200 ms before to 400 ms after the stimulus onset. The subject baseline (subject in place but no stimulation delivered) and the four stimulation runs for each subject are arranged in one column. Note the normalization is done separately for each run, and hence the sharp transient at zero is more prominent for weak signals. For easy comparison of signal strength, a gray vertical bar is added in each figurine corresponding to a stimulation run to denote the maximum signal strength in the subject baseline.

nals. For the normal subjects, the MEG signal for weak stimulation and for some of the strong foot stimulation was not evident when all 148 MEG channels were superimposed but was discernible when a subset of channels around the central sulcus was displayed. For the paraplegic subjects, foot stimulation produced a signal with no clearly discernible pattern at either

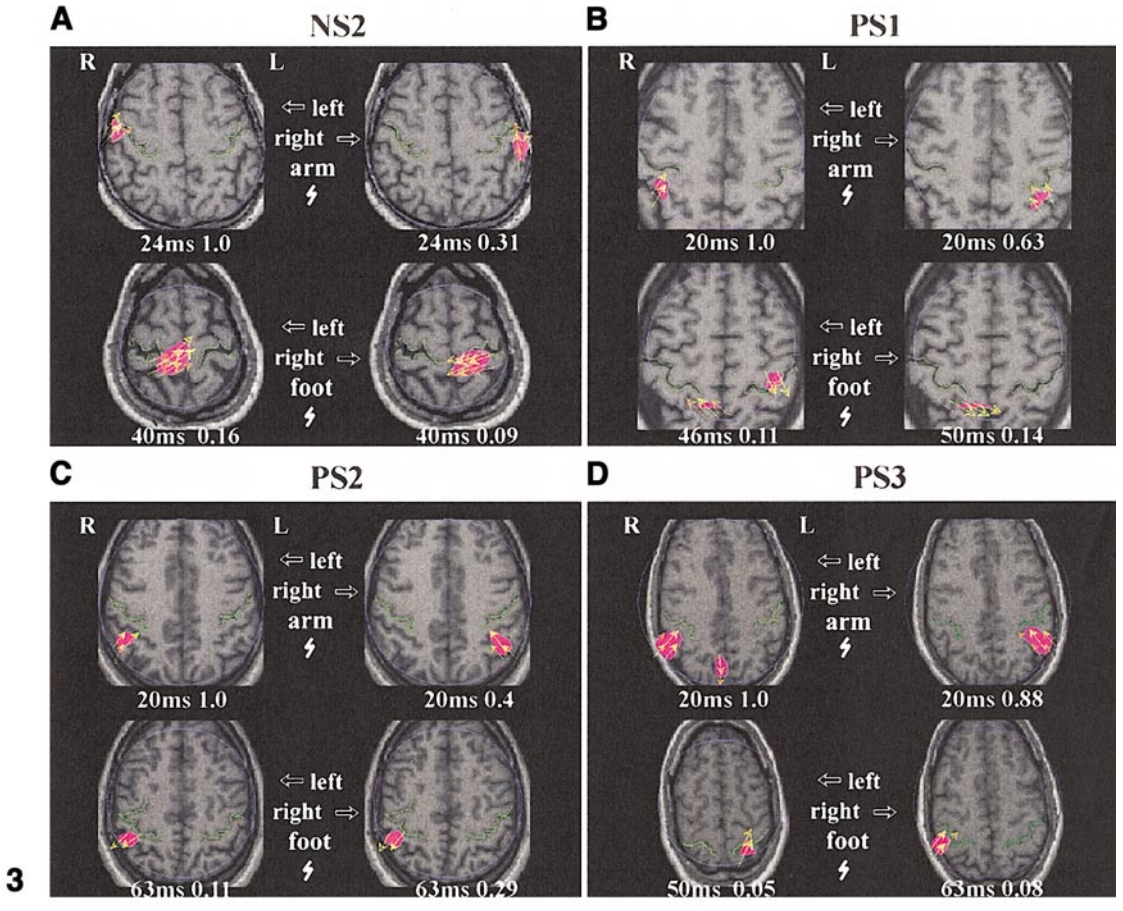

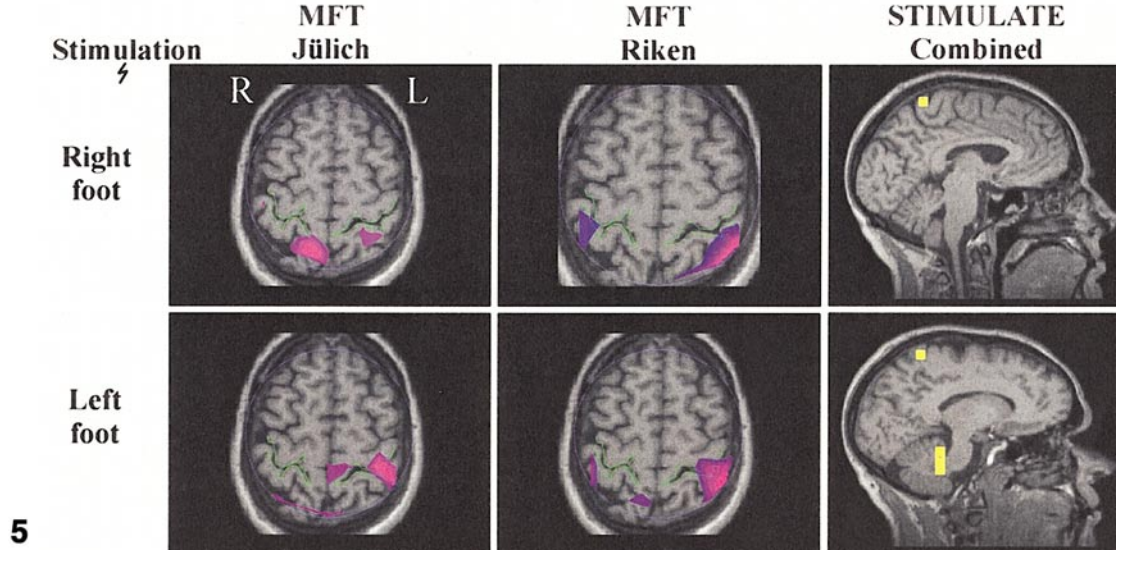

FIG. 3. Instantaneous MFT activations in the SI arm and foot areas following strong limb stimulation. The pink contour plot shows the activated areas while the arrows show the current density vector. The contour plot and arrow map for each display is normalized separately. The thin blue circles show the cut of source space at the display level and the green outline marks the central sulcus. In each display the latency is printed together with the relative maximum strength across conditions for each subject. For details, especially relating to the foot activations for paraplegic subjects see text.

FIG. 5. Using STIMULATE to combine weak activations across all four runs (strong, weak, Jülich, and Riken) following foot stimulation for paraplegic subject PS1. The top and bottom rows are for right and left foot stimulation, respectively. The first two columns show examples of weak instantaneous current density distributions behind the central sulcus following strong foot stimulation from Jülich and Riken, respectively. The third column shows the results from pixel by pixel analysis using STIMULATE with a poststimulus active period and a prestimulus baseline taken from all four runs. For the right foot stimulation a significant ($P < 0.02$) activation (yellow square) is evident on the contralateral (left) SI foot area (active period from 60 to 130 ms after stimulus onset). For the left foot stimulation an even more highly significant ($P < 0.01$) activation (yellow square) is seen for contralateral (right) SI foot area (active period from 90 to 150 ms) together with cerebellum activation.

level of stimulation. The activity behind the central sulcus higher than the pre-stimulus activity was evident between 27 and 120 ms. Such peaks had low amplitude and were no more than two times stronger than the peaks seen in the baseline runs.

Instantaneous MFT Activation in SI and SII Areas

The MFT analysis for the averaged data revealed activations in the sensorimotor area and adjacent posterior parietal area in all subjects. For strong arm stimulation, focal and strong activations were identified in the contralateral SI arm area of each of the five subjects at the expected early latency, well within 30 ms after stimulus onset. For strong foot stimulation, both normal subjects showed activations in the latency range 40–45 ms in the contralateral SI foot area. Activations were also identified in the paraplegic subjects but they were weak and intermittent. Figure 3 shows typical instantaneous MFT solutions for the strong limb stimulation for one normal subject (NS2) and the three paraplegic subjects (PS1–PS3). Among the three paraplegic subjects, only for PS1 instantaneous activity was occasionally identified at locations consistent with the normal cortical foot representation and at latencies similar to the ones encountered when activity in the foot area was observed in normal subjects. For NS1, NS2, and PS1 the amplitude of the response evoked by foot stimulation was one-tenth of that for arm stimulation. All activations in the normal subjects and only activations following arm stimulation for the paraplegic subjects were well defined in time. Activations following foot stimulation in paraplegic subjects (including the ones displayed for PS2 and PS3 in Fig. 3) were brief, erratic and weak. Without further analysis these activations were barely distinguishable from random fluctuations seen in the baseline runs. Before we give a detailed presentation of the results in terms of regional time courses (Fig. 4), we first summarize the activations following stimulation below the lesion for each paraplegic subject, as they were seen in the instantaneous MFT solutions. This overview is necessary because the activation curve analysis misses completely weak, distributed, and intermittent activity behind the central sulcus.

PS1. The left foot strong stimulation was followed by activity in the contrlateral SI foot area at 46 ms and in the ipsilateral side between 43 and 63 ms after the stimulus onset. Ipsilateral SI activity was also occasionally observed between 47 and 96 ms following left foot weak stimulation. Right foot strong stimulation was followed by activity in the contralateral SI foot area at 67 ms and in the ipsilateral SI foot area between 47 and 79 ms. Weak stimulation of the same limb was followed by the activity in the contralateral SI foot area between 43 and 79 ms and in the contralateral SII at 79 ms.

PS2. Intermittent activity behind the central sulcus around ipsilateral SI area was identified between 65 and 120ms after the stimulus onset following left foot strong stimulation and between 27 and 85 ms following left foot weak stimulation. Also, activity around 44 ms was evident on the contralateral SI area following left foot weak stimulation. For the right foot stimulation at the strong level the contralateral SI area was activated around 44 ms, and later at 93 ms after the stimulus onset. The contralateral SI and SII activity was observed at 39–46 ms and 95 ms, respectively, following the right foot stimulation at the weak level.

PS3. Ipsilateral SI activity was occasionally observed between 43 and 92 ms following left foot stimulation at the strong level, while the stimulation of the same limb at the weak level showed activity around ipsilateral SI foot area between 47 and 98 ms.

ROI Activation Curves and Post-MFT Statistics

The displays of instantaneous maps of MFT solutions only lead to a qualitative description of the results. A more quantitative analysis follows the application of the composite KS test, which allows us to assess if and when each ROI activation is significant. The strong stimulation produced stronger ROI activations with high significance at well-defined latency ranges. The activation curves for the weak stimulations were stronger than for the subject baseline runs, but considerably weaker than their counterparts for strong stimulations. The peaks in ROI activations for weak stimuli were also less sharp and appeared at later latencies than the corresponding peaks following strong stimulation. Figure 4 shows the activation curves for all six ROIs in all strong limb stimulation runs. The curves for the activations in the same ROI following ipsi- and contralateral arm or foot stimulation are grouped and normalized together to allow direct comparison. The subject baseline runs are not shown to avoid clutter in the figure, instead its maximum level is marked on each graph if it is at all discernible (see caption of Fig. 4). We describe briefly the activation in each ROI in turn.

SI arm area activations. For all five subjects a strong significant activity in the left and right SI arm area was identified within 30 ms following stimulation of the contralateral arm. For most subjects, the contralateral arm activation was followed within the next 50–70 ms by activity on the ipsilateral side at considerably lower intensity that nevertheless reached significance when compared to the subject baseline run. Foot stimulation produced weak activation in the arm area, with peak average value typically one fifth or tenth of the peak average value following arm stimulation (except for PS1 where the ratio was only 2). These weak activations reached significance only inter-

mittently and on only two brief occasions in the first 100 ms after stimulus onset, once for NS1 and once for PS3, when compared to the subject baseline runs.

SI foot area activations for normal subjects. For normal subjects at some point in the poststimulus period the left and right SI foot area was significantly active when compared to the subject baseline run when either ipsi- or contralateral stimulation was applied to the arm or foot. The activations on the contralateral side following arm and foot stimulation were comparable. Activation in the foot area following contralateral foot stimulation was either the strongest or within 12% of the strongest response.

SI foot area activations for paraplegic subjects. Significant activation of the SI foot areas was identified in each paraplegic subject following arm stimulation. For PS1 significant activation in SI foot area was identified following foot stimulation. On the right SI foot area a robust sustained activation followed contralateral (left) foot stimulation, while on the left SI foot area weak activations were observed and reached significance briefly and intermittently. For PS2 and PS3 the activations behind the central sulcus following foot stimulation were too weak and intermittent and the corresponding activation curves produced practically no statistically significant activation.

SII area activations. For both the left and right SII areas, significant activations were identified in all five subjects. In all subjects except NS2 the SII area was activated more strongly after the strong contralateral arm stimulation. For NS2, the strongest SII activation followed the ipsilateral arm stimulation. Activation in SII was identified in the poststimulus period after foot stimulation for NS2, but not in NS1. All the SII activations discussed so far followed the ones in the SI arm area as expected. Left SII activation was identified also for either foot stimulation in PS1 that reached significance for similar periods as in normal subjects. Weak SII activation that only intermittently reached significance was also identified for PS3 in both left and right hemispheres.

In summary. Foot stimulation below the clinical complete lesions produced no activation for paraplegic subject PS2, and only weak activations in PS3 who occasionally reached significance for the SI arm and SII areas, usually briefly and late in the poststimulus period. Statistically significant responses were identified for PS1 on both SI foot areas following contralateral foot stimulation. Compared to corresponding activations in the contralateral SI foot area in normal subjects, for PS1 the activation on the left reached significance rather late while on the right it sustained over 100 ms. In both cases the actual average waveform had less well-defined peaks than the corresponding average waveforms in normal subjects. Statistically significant activity was also identified in the left SII areas following stimulation of either the left or right foot of PS1, which again corresponded to signal waveforms without sharp and well-defined peaks.

Single Subject Analysis across the Two Laboratories

The activation for PS1 following foot stimulation although identifiable it was less focused in both space and time. Examples of these weak instantaneous activations are given in the first two columns of Fig. 5 from both laboratories at axial slices corresponding to the SI arm and SI foot areas. It is clearly impossible to ascertain significance by just visual inspection of the instantaneous MFT solutions. We combined all four measurements (weak and strong runs from each laboratory) in one statistical analysis using STIMULATE to identify significant activations in each first and then to combine them into one map. Surprisingly, for each foot stimulation the fuzzy instantaneous activations in each measurement lead to significant activations which were very focal, just behind the contralateral central sulcus where the SI foot area is expected to be, as shown in the third column of Fig. 5.

Figure 6 shows in detail the STIMULATE results and corresponding activation curves obtained from MFT analysis of the Jülich and RIKEN data following the arm stimulations of the paraplegic subject PS1. STIMULATE was used to identify the SI foot area (from the foot stimulation runs of Fig. 5), and the SI arm and SII areas (from the arm stimulation runs). The coordinates of the centers of these areas agreed well with the ones used for the earlier analysis of the Jülich data differing by just a few millimeters (worst cases with 8 mm difference were for right SI foot and left SI arm). The directional activations within these ROIs were then defined for these areas for all arm stimulation runs. The middle column of Fig. 6 shows MRI slices at the level of the SI foot (top), SI arm (middle), and SII (bottom) area. The extended bilateral white strip in the top middle figurine shows the extent of the strip of significant activation identified by STIMULATE when the MFT solutions from all right arm stimulation runs were compared to the subject baseline run. No such significant activation was observed with left arm stimulation. The curves on either side show the activations following strong and weak contralateral arm stimulation from the two laboratories. The agreement is very good for strong stimulation at the early latencies, and still reasonable, even for long latencies when the activation is statistically significant for both laboratories. The activations in the SI foot and SI arm areas under the same stimulation are similar but not identical.

DISCUSSION

The project was designed to explore the logistical and technical feasibility of using MEG to study the cerebral activity of patients with long-term stable posttrau-

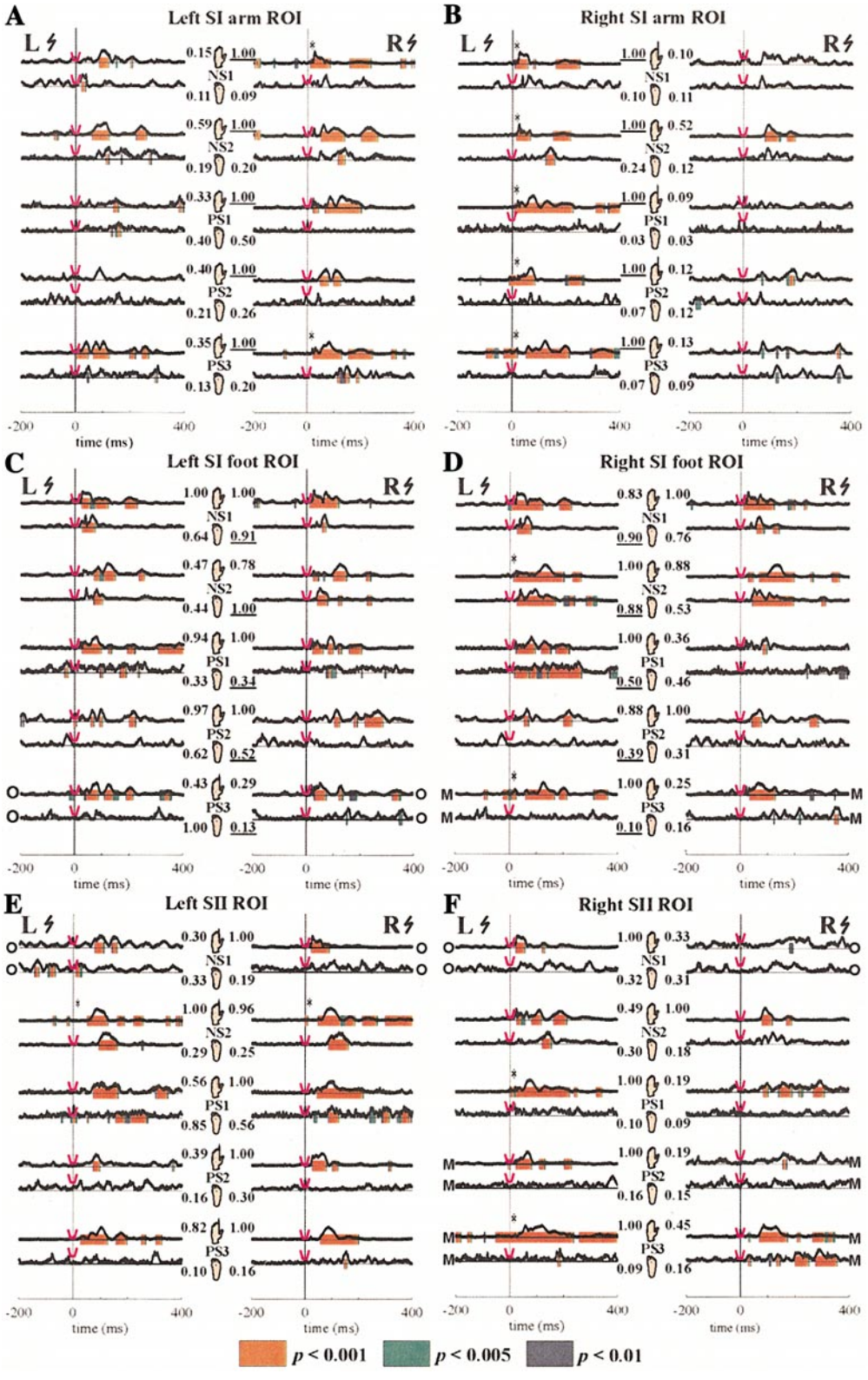

FIG. 4. The activation curves and the level of significance as given by our composite KS test for the two normal (NS1-2) and the three paraplegic (PS1-3) subjects from Jülich. Only strong stimuli are used with a hand or foot symbol indicating the stimulation site. The latency is marked as significant only if, in at least two consecutive time slices, the KS test produces $P < 0.01$. For each subject, four curves are plotted for the ROI activation following stimulation at each site and the curves are scaled so that they rise to the same maximum. The relative strengths are displayed in the figure, with the underlined value indicating the ROI best coupled to the stimulus. A V shape symbol with flat horizontal base is introduced to indicate the relative signal to noise level. The horizontal line of the symbol on the vertical axis marks the maximum value of the ROI activation from the subject baseline run. Further, a * mark is printed if the baseline signal is less than 2% of the overall maximum of the run. The letters M or O indicate, respectively, that the ROI was defined by mirroring the coordinates from the other hemisphere or by averaging the TC of the corresponding ROIs of other subjects and then back-transforming to the subject's MRI coordinates (see text for details).

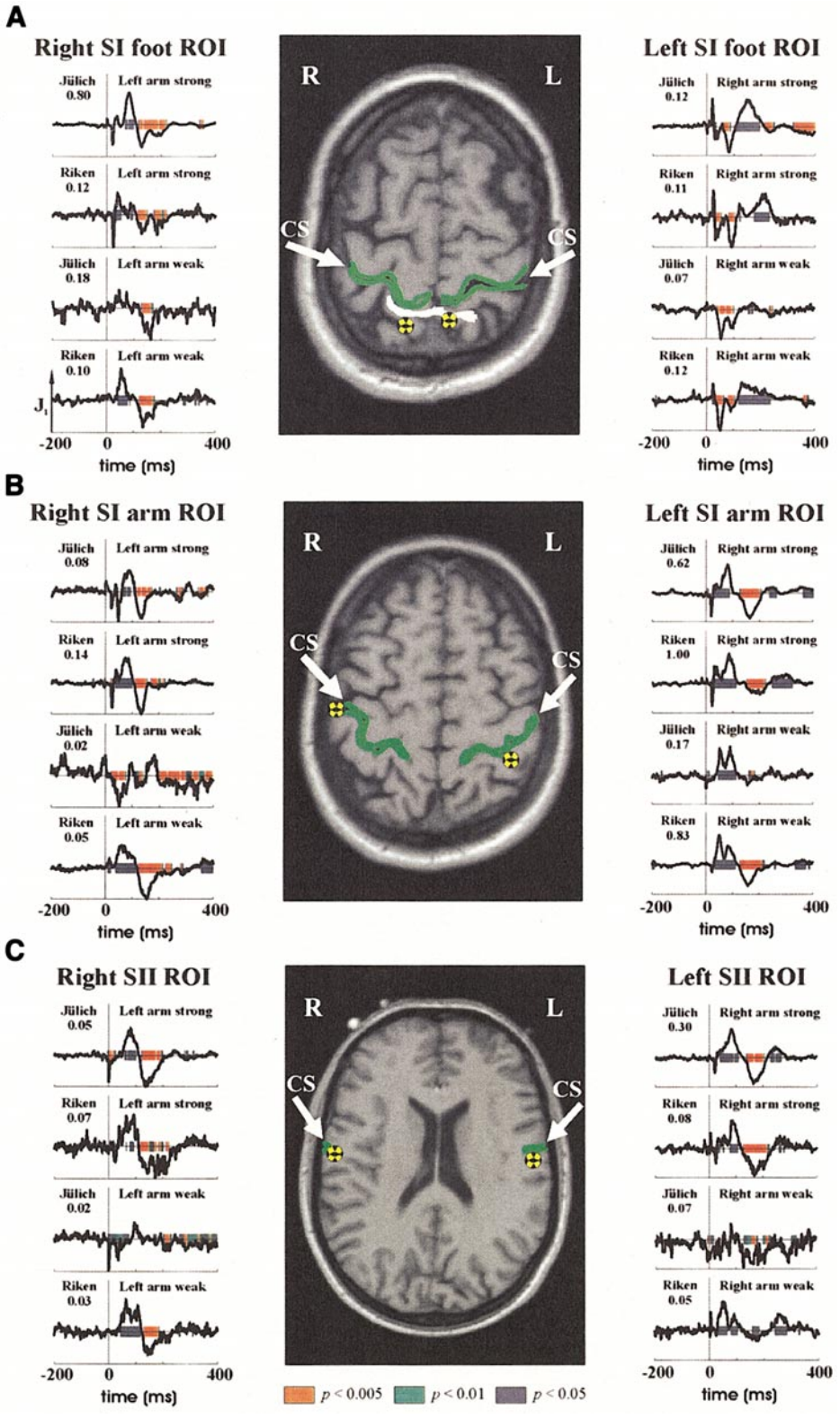

FIG. 6. Foci and time-courses of activations following arm stimulations for PS1 from the experiments in both Jülich and Riken. Figurines on the left and right columns show the respective ROI activation on the right and left hemisphere with statistical significance from the composite KS-test. The middle column show the STIMULATE results obtained by combining all four experiments (weak, strong and Jülich and Riken) using −150 to −50 ms as the baseline period. The results for three different ROIs in each hemisphere are shown for (A) SI foot area (corresponding to the inaccessible limb), (B) SI arm and (C) SII area in the top, middle and bottom rows, respectively. The central sulcus is highlighted in green with a white arrow pointing to it. The white band in the middle figurine of (A) shows the wide bilateral activity

matic spinal cord injury. Our work shows that MEG studies of paraplegic patients are indeed practical.

The analysis of the data from Jülich surprisingly revealed weak but significant activations elicited by stimulation of paraplegic subjects below what was defined to be a complete lesion. For the two normal and one paraplegic subject who produced the most consistent contralateral stimulation from the "silent" limb we repeated the measurements with a different MEG system.

We have applied MFT analysis to compute at each timeslice independently the 3-D distribution of activity throughout the brain. ROI activations were identified on functional criteria and independently confirmed by the location of the maximal activity on the MRI of each subject. The time course of activation within each ROI was computed and its significance across time was assessed by a conservative variant of the standard KS test. For normal subjects our analysis identified activations around 20–60 ms in the contralateral SI area and around 40–200 ms in the SII area. These locations and their time courses agree well with a large number of recent studies of normal subjects using stimulation of the median or tibial nerves with intracranial EEG (Allison *et al.*, 1989, 1996), MEG (Forss *et al.*, 1994; Kakigi, 1994; Kakigi *et al.*, 1995; Hari *et al.*, 1996), and fMRI (Kurth *et al.*, 1998) studies. Somatosensory stimulation elicits activity in many brain areas (Korvenoja *et al.*, 1999). In our study many of these areas were also identified, but the primary and secondary somatosensory cortices (SI and SII) were the most prominently activated areas across normal and paraplegic subjects. We decided to restrict our investigation, at least in the first instance, to these areas.

Scalp recorded somatosensory evoked potentials to stimulation of the lower extremities agrees well with diagnosis of complete paraplegia (Perot and Vera 1982). All our paraplegic subjects were diagnosed as complete by standard clinical methods including additional electrophysiological recordings performed prior to our experiments (Appendix A). Two key capabilities enabled our analysis to detect the weak and diffused activations that escaped detection in the previous tests. First, MFT allows us to cover the entire brain without any prior assumptions about the number or nature (e.g., focal or distributed) of the generators. Furthermore, weak activations can be extracted accurately in the presence of other interfering activity, as was recently demonstrated in the context of the well understood early V1 activation (Tzelepi *et al.*, 2001). Second, since the MFT analysis is performed independently for each timeslice we can use statistical analysis on the MFT solutions to enhance weak activations and disentangle them from other random events which might have survived the averaging of many trials. Two such post-MFT analysis were employed; the first relied on STIMULATE to do a pixel by pixel analysis and the second relied on identifying ROIs for the main areas and then applying our composite KS test to their activation curves. Both post-MFT statistical analysis methods were able to combine the measurements from Jülich and RIKEN in a complementary way. The composite KS tests allowed the activity within a well-defined spatial neighbourhood to be studied across all latencies. STIMULATE on the other hand allowed us to combine all runs of the same limb into maps of significant changes in activation over a predefined range of latencies covering the entire brain. This analysis when applied to normal subjects produced results of very focal nature, very similar to what one obtains with similar analysis (e.g., using t test) in PET and fMRI. In the case of foot stimulation for PS1 the MFT analysis identified activations which were broadly distributed in time and again post-MFT analysis showed very focal activations in the general area where the SI foot representation is normally found. In addition, for PS1 STIMULATE analysis of MFT solutions from all right arm stimulation runs produced very extended bilateral activation in the same general SI foot areas (Fig. 6). This result must be seen in the context of significant activations observed in the putative SI foot area when either arm was stimulated in all five subjects, especially at the strong level (Fig. 4). In the normal subjects, the activation strength in the SI foot ROI was comparable for contralateral strong arm and contralateral strong foot stimulations, whereas it was much stronger for the arm rather than the foot stimulations in the paraplegic subjects. Activations of the SI foot areas by both arm and foot stimulation is unexpected at least for normal subjects. The possibility of leakage of activity from SI arm or SMA area in the MFT solutions cannot be excluded, but it is an unlikely explanation, because for such superficial areas the MFT resolution is very good. The ability of fMRI to study single subjects have replaced the rather rigid homonculus with more widespread activations in individual subjects (Gelnar *et al.*, 1989), and much like in our case common foci across subjects identified in the classical somatosensory sites. We note that a single

identified by STIMULATE between 60 and 120 ms after stimulus onset ($P < 0.01$) following right arm stimulation. In each middle figurine yellow and black ball-like symbols show the foci identified by STIMULATE. For (A) the ROIs were defined from foot stimulation. In (B) the ROI contains pixels corresponding to $P < 0.05$ identified by STIMULATE with contralateral arm stimulation (active period from 25 to 50 ms for left SI and from 25 to 60 ms for the right SI). (C) shows the corresponding SII areas, with highly significant activity identified by STIMULATE ($P < 0.005$) for active period from 60 to 120 ms for left SII and from 50 to 110 ms for right SII. Each curve is normalized separately but the relative maximum for each curve compared to the highest value (1.0) is printed in text for easy comparison.

current dipole analysis restricted to 20–30 channels could easily produce solutions with fairly high goodness of fit with current dipoles close to the dominant SI arm area when applied to data generated by focal activations in SI arm and foot areas with relative strengths similar to the ones identified in our study.

The number of subjects studied is very small, but the rather surprising activations identified following stimulation below the complete lesions were confirmed by reexamination of one of the subjects and an extensive statistical analysis of the combined data from two different laboratories. One major goal in sight is to identify the mechanism responsible for the weak activations we observe in the cortex following stimulation below "complete" lesions with no concomitant sensation at the lower limb. Many recent studies have shown reorganisation of the somatosensory areas following acute injury at the periphery. In a recent study (Green *et al.*, 1999) a correlation was found between the posterior reorganisation following injury and prognosis which may be the consequence of preferential survival of axons originating in somatosensory cortex and contribute to the corticospinal tract. In a more recent fMRI and TMS study (Foltys *et al.*, 2000) demonstrated that the plegic hand was still represented in the motor cortex, despite the fact that the same cortical area was activated too by movements of the nonplegic muscles. It is possible that the lesion is not really complete and that all we see is the effect of a few nerves that still function across the lesion. Our study points to the intriguing alternative that an imprecise communication may be preserved between the cortex and the body below what is a complete lesion (based on standard clinical tests). Such a mechanism cannot be excluded *a priori*, since the body below the lesion is still connected to the rest and supplied by blood and nutrients. It is well known that other pathways exist, possibly the spino thalamic tract, or the spino reticular pathway (less likely for PS1 as it sends information bilaterally) may have conducted information to the cortex but not into consciousness. Autonomic fibers also ascend in the cord and are related to sweating, blood pressure etc, but it is unlikely that these are involved as the response of the sensory cortex is so focal. The most likely fibers are those spinal pathways to the cerebellum, thalamus and reticular formation all of which send information to the cortex. Clearly more subjects should be examined in this way under strict clinical conditions which were not available in either of the two MEG laboratories. Whatever the mechanism is, understanding it may eventually lead to ways of enhancing any remaning sensation with appropriate training.

APPENDIX A

The patients studied by MEG underwent clinical and neurophysiological examination for research purposes in 1997 (prior to their MEG examination). This was additional to their normal clinical tests performed earlier.

Clinical tests. Clinical neurological examination was performed according to International Standards for Neurological and Functional Classification of Spinal Cord Injury (Maynard *et al.*, 1997). Motor function was tested in 10 key muscles for myotomes C5 to T1 and L2 to S1 on each side of the body and graded from 0 to 5. Sensory function was tested for light touch (principally testing posterior columns) and pin-prick (principally testing spino-thalamic pathways) on 28 key-points for dermatomes C2 to S4/5 on each side of the body and graded 0 to 2. Total motor (maximum 100) and sensory (maximum 112) scores were derived by adding up all motor and sensory grades.

In all three paraplegic subjects the upper limb motor function was normal, while there was no voluntary motor function in the lower limbs (total motor score was 50 in all three subjects). The sensory function was normal down to the last normal spinal segment as stated above (between T6 and T11) with complete loss of sensation for both tested modalities below the level of spinal cord injury (total sensory scores between 52 and 72).

Electrophysiological tests. Motor evoked potentials (MEP) were recorded from biceps brachii, abductor pollicis brevis, quadriceps femoris, and tibialis anterior muscles using self-adhesive surface electrodes, in response to transcranial magnetic stimulation (TMS) over the vertex with 1.5 Tesla Magstim 200 magnetic stimulator. Stimulus intensity was gradually increased until a MEP was obtained or the maximal stimulator output of 100% was reached. EMG signals were analyzed on Medelec Sapphire II, filter settings were 3–10 kHz, analysis period 50 ms for upper limbs and 100 ms for lower limbs.

Somatosensory-evoked potentials (SSEP) were performed on Medelec Sapphire II. Upper extremity SSEPs were recorded over the sensory cortex from C3 and C4, reference Fz, in response to median nerve stimulation at the wrist. Stimulus intensity was just greater than motor threshold, stimulus duration 0.1 ms, repetition rate 5 Hz, filter settings 10–3 kHz, analysis period 50 ms and number of averaged responses 1024. Lower extremity SSEPs were recorded from Cz, reference Fz, in response to posterior tibial nerve stimulation at the ankle with maximal stimulus intensity of the EMG machine of 100 mA, stimulus duration 0.1 ms, repetition rate 5 Hz, filter settings 10 Hz–2 kHz, analysis period 100 ms and number of averaged responses 1024. SSEP and MEP latencies, durations and amplitudes of both upper extremities' responses were within normal limits for all three paraplegic subjects.

In all three subjects no responses could be observed nor recorded from either lower limb, using the maximal

Magstim magnetic stimulator stimulus intensity of 100% for motor evoked potentials, and the maximal stimulus intensity of 100 mA of Medelec Sapphire EMG machine for somatosensory evoked potentials.

Thus, on the basis of the tests performed, neurophysiologically, as well as clinically, all three paraplegic subjects appeared to have a complete thoracic spinal cord lesion.

ACKNOWLEDGMENTS

We thank our paraplegic subjects for their participation in this study. The first MEG experiment was performed in Research Center Jülich, Germany, and the data were analyzed at RIKEN, Japan. The study was also supported financially by the Sir Jimmy Savile Trust for Stoke Mandeville Hospital and The X Appeal grants of The Royal College of Radiologists, London (UK). Dr. G. Savic performed the electrophysiological tests and provided the details from the Stoke Mandeville Hospital archive. R.B. acknowledges Mr. P. Teddy, FRCS, and Dr. P. Anslow, FRCR (Radcliffe Infirmary, Oxford) for help with the initial discussions. We thank Dr P. Fenwick for helpful discussions and useful comments on the final manuscript.

REFERENCES

Alexeeva, N., Broton, J. G., Suys, S., and Calancie, B. 1997. Central cord syndrome of cervical spinal cord injury: Widespread changes in muscle recruitment studied by voluntary contractions and transcranial magnetic stimulation. *Exp. Neurol.* **148**(2): 399–406.

Alexeeva, N., Broton, J. G., and Calancie, B. 1998. Latency of changes in spinal motoneuron excitability evoked by transcranial magnetic brain stimulation in spinal cord injured individuals. *Electroencephalogr. Clin. Neurophysiol.* **109**(4): 297–303.

Allison, T., McCarthy, G., Wood, C., Williamson, P., and Spencer, D. 1989. Human cortical potentials evoked by stimulation of the median nerve. II. Cytoarchitectonic areas generating long-latency activity. *J. Neurophysiol.* **62:** 711–722.

Allison, T., McCarthy, G., Luby, M., Puce, A., and Spencer, D. 1996. Localization of functional regions of human mesial cortex by somatosensory evoked potential recording and by cortical stimulation. *Electroencephalogr. Clin. Neurophysiol.* **100:** 126–140.

Bruehlmeier, M., Dietz, V., Leenders, K. L., Roelcke, U., Missimer, J., and Curt, A. 1998. How does the human brain deal with a spinal cord injury? *Eur. J. Neurosci.* **10**(12): 3918–3922

Calancie, B., Alexeeva, N., Broton, J. G., Suys, S., Hall, A., and Klose, K. J. 1999. Distribution and latency of muscle responses to transcranial magnetic stimulation of motor cortex after spinal cord injury in humans. *J. Neurotrauma* **16**(1): 49–67.

Foltys, H., Kemeny, S., Krings, T., Boroojerdi, B., Sparing, R., Thronn, A., and Töpper, R. 2000. The representation of the plegic hand in the motor cortex: a combined fMRI and TMS study. *NeuroReport* **11:** 147–150.

Forss, N., Hari, R., Salmelin, R., Ahonen, A., Hämäläinen, M., Kajola, M., Knuutila, J., and Simola, J. 1994. Activation of the human posterior parietal cortex by median nerve stimulation. *Exp. Brain Res.* **99:** 309–315.

Gelnar, P. A., Krauss, B. R., Szeverenyi, N. M., and Apkarian, A. V. 1998. Fingertip representation in the somatosensory cortex: An fMRI study. *NeuroImage* **7:** 261–283.

Green, J. B., Sora, E., Bialy, Y., Ricamato, A., and Thatcher, R. W. 1998. Cortical sensorimotor reorganization after spinal cord injury: an electroencephalographic study. *Neurology* **50**(4): 1115–1121.

Green, J. B., Sora, E., Bialy, Y., Ricamato, A., and Thatcher, R. W. 1999. Cortical motor reorganization after paraplegia: an EEG study. *Neurology* **53**(4): 736–743.

Hari, R., Nagamine, T., Nishitani, N., Mikuni, N., Sato, T., Tarkiainen, A., and Shibasaki, H. 1996. Time-varying activation of different cytoarchitectonic areas of the human SI cortex after tibial nerve stimulation. *NeuroImage* **4:** 111–118.

Ioannides, A. A., Bolton, J. P. R., and Clarke, C. J. S. 1990. Continuous probabilistic solutions to the biomagnetic inverse problem. *Inverse Problem* **6:** 523–542.

Ioannides, A. A., Muratore, R., Balish, M., and Sato, S. 1993a. *In vivo* validation of distributed source solutions for the biomagnetic inverse problem. *Brain Topogr.* **5:** 263–273.

Ioannides, A. A., Singh, K. D., Hasson, R., Baumann, S. B., Rogers, R. L., Guinto, F. C., and Papanicolaou, A. C. 1993b. Comparison of current dipole and magnetic field tomography analyses of the cortical response to auditory stimuli. *Brain Topogr.* **6:** 27–34.

Ioannides, A. A. 1995a. Estimates of 3D brain activity ms by ms from biomagnetic signals: method (MFT), results and their significance. In *Quantitative and Topological EEG and MEG Analysis* (E. Eiselt, U. Zwiener, and H. Witte, Eds.), pp. 59–68. Universitätsverlag Druckhaus-Maayer GmbH, Jena.

Ioannides, A. A., Liu, M. J., Liu, L. C., Bamidis, P. D., Hellstrand, E., and Stephan, K. M. 1995b. Magnetic field tomography of cortical and deep processes: Examples of "real-time mapping" of averaged and single trial MEG signals. *Int. J. Psychophysiol.* **20:** 161–175.

Kakigi, R. 1994. Somatosensory evoked magnetic fields following median nerve stimulation. *Neurosci. Res.* **20:** 165–174.

Kakigi, R., Koyama, S., Hoshiyama, M., Shimojo, M., Kitamura, Y., and Watanabe, S. 1995. Topography of somatosensory evoked magnetic fields following posterior tibial nerve stimulation. *Electroencephalogr. Clin. Neurophysiol.* **95:** 127–134.

Keirstead, H. S. and Blakemore, W. F. 1999. The role of oligodendrocytes and oligodendrocyte progenitors in CNS remyelination. *Adv. Exp. Med. Biol.* **468:** 183–197.

Korvenoja, A., Huttunen, J., Salli, E., Pohjonen, H., Martinkauppi, S., Palva, J. M., Lauronen, L., Virtanen, J., Ilmoniemi, R. J., and Aronen, H. J. 1999. Activation of multiple cortical areas in response to somatosensory stimulation: combined magnetoencephalographic and functional magnetic resonance imaging. *Hum. Brain Mapp.* **8:** 13–27.

Kurth, R., Villringer, K., Mackert, B. M., Schwiemann, J., Braun, J., Curio, G., Villringer, A., and Wolf, K. J. 1998. fMRI assessment of somatotopy in human Brodmann area 3b by electrical finger stimulation. *NeuroReport* **9:** 207–212.

Levy, W. J., Jr, Amassian, V. E., Traad, M., and Cadwell, J. 1990. Focal magnetic coil stimulation reveals motor cortical system reorganized in humans after traumatic quadriplegia. *Brain Res.* **510**(1): 130–134.

Liu, L. C., Ioannides, A. A., and Taylor, J. G. 1998. Observation of quantization effects in human auditory cortex. *NeuroReport* **9:** 2679–2690.

Liu, L. C., Ioannides, A. A., and Streit, M. 1999. Single trial analysis of neurophysiological correlates of the recognition of complex objects and facial expressions of emotion. *Brain Topogr.* **11:** 291–303.

Lotze, M., Laubis-Herrmann, U., Topka, H., Erb, M., and Grodd, W. 1999. Reorganization in the primary motor cortex after spinal cord injury—A functional Magnetic Resonance (fMRI) Study. *Restor. Neurol. Neurosci.* **14:** (2–3) 183–187.

Maynard, F. M. Jr, Bracken, M. B., Creasey, G., Ditunno, J. F. Jr, Donovan, W. H., Ducker, T. B., Garber, S. L., Marino, R. J., Stover, S. L., Tator, C. H., Waters, R. L., Wilberger, J. E., and Young, W. 1997. International standards for neurological and functional classification of spinal cord injury. *Spinal Cord* **35:** 266–274.

McDonald, J. W. 1999. Repairing the damaged spinal cord. *Sci. Am.* **281**(3): 64–73.

Nicholls, J. G., Adams, W. B., Eugenin, J., Geiser, R., Lepre, M., Luque, J. M., and Wintzer, M. 1999. Why does the central nervous system not regenerate after injury? *Surv. Ophthalmol.* **43** (Suppl 1): S136–141.

Perot, P. L. Jr and Vera, C. L. 1982. Scalp-recorded somatosensory evoked potentials to stimulation of nerves in the lower extremities and evaluation of patients with spinal cord trauma. *Ann. N.Y. Acad. Sci.* **388:** 359–368.

Roelcke, U., Curt, A., Otte, A., Missimer, J., Maguire, R. P., Dietz, V., and Leenders, K. L. 1997. Influence of spinal cord injury on cerebral sensorimotor systems: A PET study. *J. Neurol. Neurosurg. Psychiatry* **62**(1): 61–65.

Smith, H. C., Davey, N. J., Savic, G., Maskill, D. W., Ellaway, P. H., Jamous, M. A., and Frankel, H. L. 2000. Modulation of single motor unit discharges using magnetic stimulation of the motor cortex in incomplete spinal cord injury. *J. Neurol. Neurosurg. Psychiatry* **68**(4): 516–520.

Streletz, L. J., Belevich, J. K., Jones, S. M., Bhushan, A., Shah, S. H., and Herbison, G. J. 1995. Transcranial magnetic stimulation: Cortical motor maps in acute spinal cord injury. *Brain Topogr.* **7**(3): 245–250.

Strupp, J. P. 1996. Stimulate. A GUI based fMRI Analysis Software Package. *NeuroImage* **3**(3): 607.

Taylor, J. G., Ioannides, A. A. and Müller-Gärtner, H. W. 1999. Mathematical analysis of lead field expansions. *IEEE Trans. Med. Imag.* **18:** 151–163.

Topka, H., Cohen, L. G., Cole, R. A. and Hallett, M. 1991. Reorganization of corticospinal pathways following spinal cord injury. *Neurology* **41**(8): 1276–1283.

Tzelepi, A., Ioannides, A. A. and Poghosyan, V. 2001. Early (N70) neuromagnetic signal topography and striate and extrastriate generators following pattern onset quadrant stimulation. *NeuroImage* **13:** 702–718.

Whittemore, S. R. 1999. Neuronal replacement strategies for spinal cord injury. *J. Neurotrauma* **16**(8): 667–673.